Hidden Properties of Carbon Dots Revealed After HPLC Fractionation

ARTICLE *in* JOURNAL OF PHYSICAL CHEMISTRY LETTERS · JANUARY 2013

Impact Factor: 7.46 · DOI: 10.1021/jz301911y

8 AUTHORS, INCLUDING:

Allen Bourdon
University of Tennessee
2 PUBLICATIONS **35** CITATIONS
SEE PROFILE

Barbara Foster
Roswell Park Cancer Institute
97 PUBLICATIONS **4,585** CITATIONS
SEE PROFILE

Luis A Colón
University at Buffalo, The State University of N…
80 PUBLICATIONS **2,275** CITATIONS
SEE PROFILE

THE JOURNAL OF PHYSICAL CHEMISTRY Letters

Letter

pubs.acs.org/JPCL

Hidden Properties of Carbon Dots Revealed After HPLC Fractionation

John C. Vinci,[†] Ivonne M. Ferrer,[†] Steven J. Seedhouse,[‡] Allen K. Bourdon,[†] Justin M. Reynard,[†] Barbara A. Foster,[‡] Frank V. Bright,[†,§] and Luis A. Colón*[,†,§]

[†]Department of Chemistry, Natural Sciences Complex, University at Buffalo, The State University of New York, Buffalo, New York 14260, United States

[‡]Department of Pharmacology, Roswell Park Cancer Institute, Buffalo, New York 14263, United States

[§]Materials Science and Engineering Program, Natural Sciences Complex, University at Buffalo, The State University of New York, Buffalo, New York 14260, United States

Supporting Information

ABSTRACT: Carbon dots (C-dots) are often synthesized, modified, and studied as a mixture. Unfortunately, the spectroscopic and biological properties measured for such C-dots assume that there is a high degree of homogeneity in the produced sample. By means of high-resolution separation techniques, we show that "as-synthesized" C-dots exist as a relatively complex mixture and that an unprecedented reduction in such complexity can reveal fractions of C-dots with unique luminescence properties. The wavelength-dependent photoluminescence commonly assigned as an inherent property of C-dots is not present in fractionated samples. While ultraviolet−visible absorption profiles reported for C-dots are typically featureless, we have found fractions of C-dots possessing unique absorption bands, with different fractions possessing specific emission wavelengths. Furthermore, fractionated C-dots showed profound differences in emission quantum yield, allowing for brighter C-dots to be isolated from an apparent low quantum yield mixture. These more luminescent fractions of C-dots displayed improved biological compatibility and usefulness as cellular imaging probes.

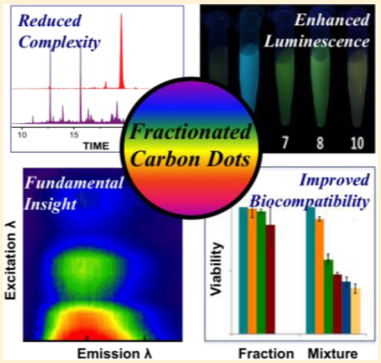

SECTION: Physical Processes in Nanomaterials and Nanostructures

Various carbon-based starting materials, such as soot,[1−3] carbohydrates,[4,5] activated carbons,[6,7] and graphite[8,9] have been reported in recent years as precursors to luminescent, carbon-based nanomaterials using straightforward oxidizing conditions at elevated temperatures. These nanomaterials have been proposed as alternatives to other nanomaterials (e.g., semiconductor quantum dots) and boast a variety of benefits such as enhanced biocompatibility and smaller sizes.[10] These so-called carbon dots (C-dots) are generally described as nanocrystalline (graphitic) or amorphous in nature, pseudospherical, and of low nanometer dimensions.[11] Graphene quantum dots (GQDs), a nanometer-scale graphene derivative where quantum confinement[12] and edge effects[13,14] introduce a bandgap, have been reported to be comparable[10] to C-dots and have similar dimensions, photoluminescence properties, surface characteristics, and biological applications.[15] There exists a continuum of species, starting with single-layer GQDs,[15,16] moving to multilayer GQDs[17,18] and finally to C-dots,[19,20] all of which can have similar dimensions and structure but generally differ in their height profiles determined by atomic force microscopy (AFM). Due to these similarities as well as the initial synthetic precursors and conditions reported for the production of C-dots[8,9,21,22] and GQDs,[1,17,23] there is often no clear distinction between these nanomaterial classes, especially when comparing multilayer GQDs to C-dots.

Wavelength-dependent emission has been reported extensively for both C-dots[4−6,9,24−27] and GQDs,[15,18,23,28−30] which is typically described as an intrinsic property of these carbon nanoparticles (CNPs).[11] Although their emission properties are not completely understood,[8,9,15,26,31] the photoluminescence quantum efficiency has been enhanced by surface passivation[5,6,27,32] and more recently by postsynthetic reduction reactions.[9,17,31] We have been interested in studying nonmodified, as-synthesized CNPs created during a typical top-down CNP synthesis by means of high-resolution separation techniques.[2,3] Clearly, multiple species are formed, and size-based separations are not sufficient to resolve the many different components in a CNP mixture.[33] For example, a size-based density gradient ultracentrifugation separation of luminescent graphene oxide yielded nanomaterial fractions with constituents exhibiting various dimensions but with similar electronic properties.[34] A small size-distribution of particles does not necessarily take into account or reflect the nanomaterial surface complexity, which can play a significant role in its properties. For example, inhomogeneity in nanographene oxide samples precluded accurate quantum yield measurements even after size-based separation. Improving

Received: November 21, 2012
Accepted: December 26, 2012
Published: December 26, 2012

the accuracy of such measurements may in fact require extensive advances in the separation of such CNPs.[34] As it was pointed out in a recent Perspective article in *The Journal of Physical Chemistry Letters*,[33] new purification techniques are necessary to realize the potential of graphene quantum dot synthesis and understanding.[33]

Recently, it has been suggested that C-dot core and surface states are separately emissive and, in combination, are responsible for the broad emission profile typically observed for a given synthesis. Further, a weak exciton−phonon coupling was found to be responsible for temperature-dependent emission properties of C-dots.[35] By creating small GQDs by a solution-chemistry synthesis, a model has been derived and experimentally confirmed indicating that size, surface and defects are all critical to the emission properties of these materials.[36] Various physical properties of C-dots and GQDs have been studied lately and include emission upconversion,[37] interaction with γ-irradiation in different solvents,[38] and thermoelectric properties.[39] Although gel electrophoresis[1] and column chromatography[9,32] have been used to obtain reduced complexity fractions of luminescent CNPs, high-resolution separation and purification methods have not been adequately applied to GQD and C-dot mixtures. As a result, the vast majority of reported studies on CNPs are performed on a multicomponent system in which a plethora of species coexists. Measurements of physical properties of CNPs would be greatly improved in accuracy and understanding by studying fractions simplified with respect to surface and size; important properties such as surface functionality, absorption/emission photoluminescent characteristics (e.g., wavelength-dependent emission), emission quantum yield (QY), magnetic properties, size, and biological compatibility are inevitably a weighted average of the many components and chemistries within the mixture. Improved high-resolution separation techniques for CNPs are needed to guide future understanding, development, and regulatory approval of CNP-based applications.[40] To address these needs, we analyzed and fractionated luminescent CNP mixtures with a high-resolution separation technique, namely, anion-exchange (AE) high-performance liquid chromatography (HPLC), which allowed us to obtain fractions with refined and unique properties not apparent by studying the unseparated mixture alone.

Luminescent CNPs were produced from graphite nanofibers shown in the Supporting Information (SI) Figure S-1, after modification of an oxidation procedure previously used to synthesize nanographene oxide stabilizers for other nanomaterials.[41] The resulting carbon material was filtered and dialyzed, preserving the 1−50 kDa superfraction (i.e., CNP mix). The CNP mix was injected onto a semipreparative AE-HPLC column, which resolved the mixture into multiple components; the separated components were monitored via ultraviolet (UV) absorption and laser-induced photoluminescence (LIP) detection (Figure 1A). Isolated fractions were collected over multiple injections as 12 individual fractions based on the LIP detection signal; milligram CNP quantities were obtained for various fractions. The production of CNPs was reproducible as indicated by similar chromatograms for multiple syntheses from a single source of starting material (cf., SI Figure S-2). When the starting material was changed, even for a different batch from the same manufacturer, the oxidation treatment required reoptimization to obtain similar chromatograms. For example, after modifying the procedure and using

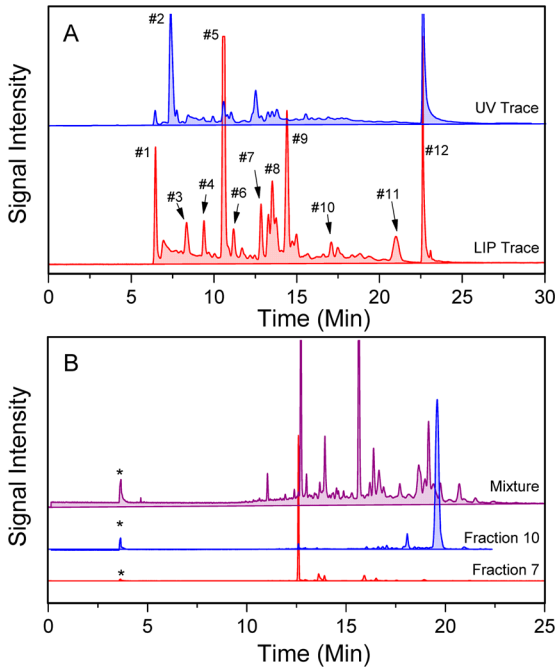

Figure 1. (A) AE-HPLC chromatograms of the 1−50 kDa mixture of our CNPs monitored by UV absorption at 250 nm and LIP (λ_{ex} = 325 nm, luminescence collected through 350 nm long pass filter). (B) Electropherograms of the CNP mix and of HPLC-collected fractions 7 and 10, monitored via LIP (λ_{ex} = 488 nm, luminescence collected through a 520 nm band-pass filter). The electroosmotic flow (EOF) marker is identified with an asterisk. See SI for the AE-HPLC and CE experimental details.

micrometer-sized carbon fibers, the similarity between chromatograms was remarkable (cf., SI Figure S-3).

The fractionation process allowed us to isolate highly photoluminescent nanomaterials relative to the unfractionated mixture. Of the 12 fractions isolated, we focused on fractions 5, 7, 8, and 10 because these fractions showed striking color differences in comparison to all other fractions and the CNP mix (SI Figure S-4); these fractions also showed the highest QY. Using rhodamine 6G as a standard, we estimated QYs for the two brightest fractions to be 6% and 7% for fractions 7 and 8, respectively, while the unfractionated CNP mixture showed an apparent QY of only 1%. It is important to note that QYs for nonmodified, as-synthesized CNP mixtures produced by oxidation of carbon-based precursors have been reported to be between 0.3 and 2%.[1,5,6,8−10,21,42] Our results suggest that there appears to be absorbing species in the mixture that do not exhibit appreciable photoluminescence. Through isolation of fractions 7 and 8 in our sample, highly luminescent species are obtained from the mixture that show 5−6 times higher QY in comparison to the mixture. A summary of the QY for the four fractions studied and the CNP mix is provided in SI Table S-1.

Examination of selected HPLC fractions by capillary electrophoresis (CE) revealed relatively simple electropherograms of species with high electrophoretic mobility when monitoring the photoluminescence after laser excitation at 488 nm (Figure 1B) and 325 nm (SI Figure S-5). The electropherograms demonstrated that each HPLC fraction collected was composed of one predominant species, indicative of an unprecedented reduction in sample complexity of the CNP mix with excellent charge/size homogeneity. Such fractions open the door for new C-dot applications such as a

dx.doi.org/10.1021/jz301911y | J. Phys. Chem. Lett. 2013, 4, 239−243

separations-based sensor,[43] which is not feasible when using multicomponent CNP mixtures. The HPLC fractionation and reduction in complexity allowed for further detailed studies of fractions and the opportunity to gain insight that may not be apparent by studying the CNP mix alone.

Transmission electron microscopy (TEM) images of fractions 7 and 10 (Figure 2) and fractions 5 and 8 (SI Figure S-6) revealed unique CNP particle sizes and distributions. The fractions showed different particle size distributions with average diameters of 7.1 ± 0.6 nm (fraction 7), 9.4 ± 0.5 nm (fraction 10), 10.1 ± 0.8 nm (fraction 5), and 14 ± 1 nm (fraction 8); average diameters are reported at the 99% confidence interval. Measurements by AFM on fractions 7 and 10 revealed heights around 5 nm (SI Figure S-7), similar to what has been reported for multilayer GQDs[17] and C-dots.[19] We note that no size-dependent trends in the optical properties of our collected fractions were observed.

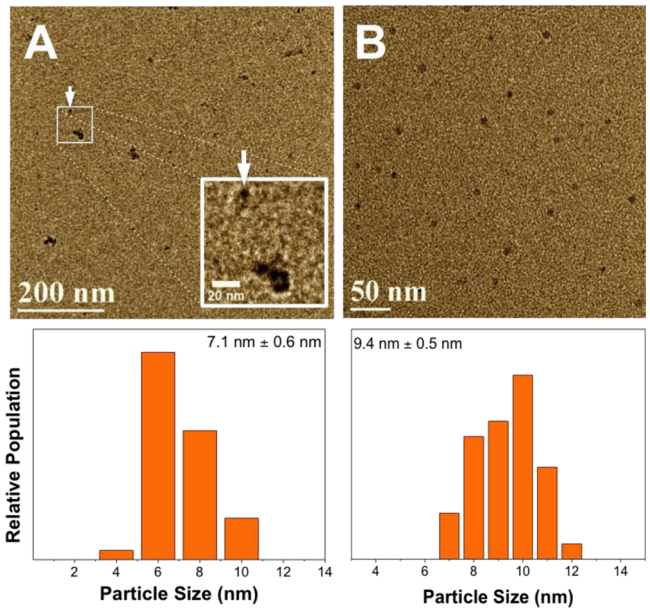

Figure 2. TEM images of (A) fraction 7 and (B) fraction 10 derived from HPLC fractionation. Some aggregation was observed in fraction 7 (selected area box) as well as isolated C-dots (indicated by arrow). The inset in panel A shows a digitally magnified example of an aggregate and an isolated C-dot from fraction 7. Size distribution for each fraction is illustrated by the bar chart below each TEM image. Average diameters are reported with their 99% confidence interval.

Reports on C-dots and GQDs displaying wavelength-independent emitted luminescence are uncommon.[9,17] The overwhelming majority of reports show wavelength-dependent emission properties for these nanomaterials, which is thought to arise from quantum confinement effects and/or different emissive trap states on particles.[11] Our spectroscopic studies of the individual fractions suggest that the typically reported wavelength-dependent emission properties of small, luminescent CNPs are not necessarily an inherent property of these nanoparticles. While the CNP mix showed wavelength-dependent luminescence emission, collected fractions did not necessarily display this property. The luminescence of the CNP mixture was multicomponent in nature, while the emission of the separated fractions appeared much narrower and less complex. Figure 3A and SI Figure S-8A highlight the multicomponent nature and broad emission profile of the

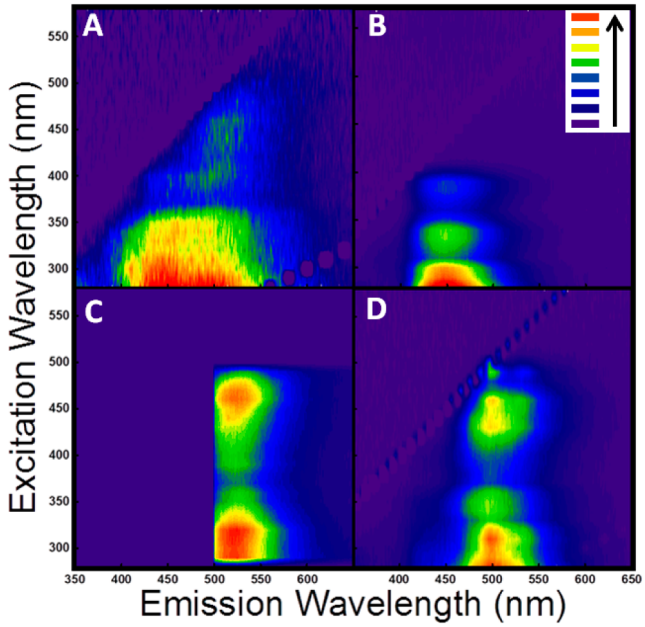

Figure 3. Excitation–emission matrices for (A) the CNP mixture, (B) fraction 5, (C) fraction 7, and (D) fraction 8. Note that analysis of fraction 7 used a 495 nm long-pass filter. The legend indicates increasing emission intensity along the direction of the arrow.

CNP mixture. The spectra for fractions 5, 7, and 8 showed significantly narrower emission profiles, each centered around a unique wavelength of approximately 450, 525, and 500 nm, respectively (Figure 3). Clearly, the unseparated mixture showed a shift to higher emission wavelengths with higher excitation wavelengths, whereas fractions 5, 7, and 8 do not display this property, which is further illustrated for fraction 7 in SI Figure S-8B. The emission spectra for fraction 10, nevertheless, showed a small red shift as a function of excitation wavelength (SI Figure S-9). Interestingly, however, the electrophoretic peak associated with fraction 10 is broader in comparison to the other fractions. It is possible that fraction 10 may still be a mixture of several species having very similar charged properties but with different spectroscopic characteristics.

It has been surmised that the isolation of C-dots with unique absorption bands and emission wavelengths could have "potentially far-reaching implications."[32] UV–visible absorption spectra for the four fractions collected revealed unique absorption bands for each fraction (SI Figure S-10). This is in contrast to the mostly featureless profile for the CNP mixture, which is typical for unseparated mixtures of C-dots[21] and GQDs.[17] Further, we show that there are unique emissive absorption bands as the luminescence excitation spectra show different excitable bands from fraction to fraction (SI Figure S-10). Fractions within a CNP mixture do indeed contain unique absorption features, which lend themselves to unique emission characteristics.

Because of the possible implications of using the fractionated CNPs in biological imaging applications, we explored the potential toxicity of the fractions using the CellTiter-Fluor cell viability assay and uptake with confocal microscopy. First, in a phagocytic cell line (RAW264.7 macrophages) expected to actively uptake the CNPs, we observed uptake (SI Figure S-11) and variable toxicity (data not shown). Next, we evaluated the uptake and toxicity profile in a nonphagocytic cell type of

dx.doi.org/10.1021/jz301911y | J. Phys. Chem. Lett. 2013, 4, 239–243

epithelial origin (TRAMP C2D mouse prostate adenocarcinoma cells) and still observed uptake (SI Figure S-12) and variable toxicity, with the higher QY fractions we studied showing markedly *less* toxicity in comparison to the mixture (Figure 4).

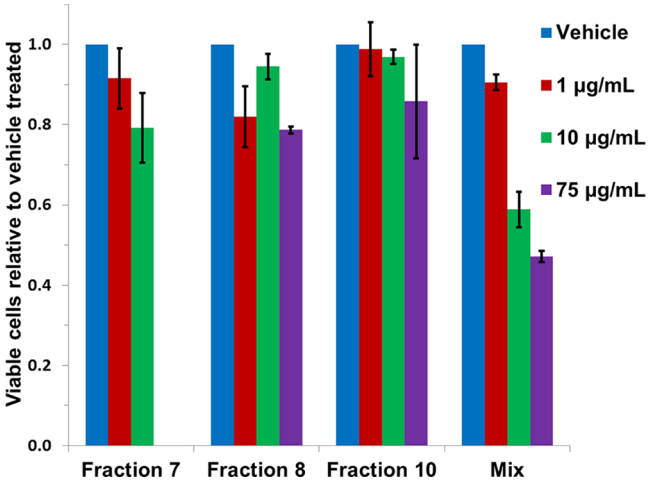

Figure 4. Cell viability of TRAMP C2D mouse prostate adenocarcinoma cells treated with various concentrations of fractionated CNPs and the CNP mix. Values of viable cells are normalized to the vehicle (water) control, which is shown for each group. Error bars represent the standard error of the mean.

In summary, we have shown that as-synthesized CNPs derived from graphite nanofibers exist in a complex mixture and that this complexity can be reduced significantly by high-resolution AE-HPLC fractionation. Fractionation via HPLC revealed CNPs with very unique absorption and emission characteristics, which would have been otherwise missed by studying the complex mixture alone. It is particularly interesting to find that fractionated C-dot components do not display wavelength-dependent emission, a characteristic that is often attributed as an intrinsic property of luminescent C-dots and GQDs. Fractionation into a single entity, as revealed by CE, opens the door for new applications of C-dots. Isolated fractions of CNPs were also less toxic to TRAMP C2D cells in comparison to the CNP mixture and were suitable for live cell imaging without further modification after synthesis. We emphasize the importance of the fractionation process when studying nanomaterials, whether luminescent or otherwise, to properly evaluate the material's characteristics. Isolation from what can be a rather complicated mixture is critical to properly assess fundamental properties of nanomaterials before establishing their applicability.

■ ASSOCIATED CONTENT

Ⓢ Supporting Information

Additional information is provided for the experimental procedures and methods. In addition, the SI includes electron microscopy images, chromatograms, electropherograms, AFM images, and spectroscopic data. This material is available free of charge via the Internet at http://pubs.acs.org.

■ AUTHOR INFORMATION

Corresponding Author

*E-mail: lacolon@buffalo.edu.

Notes

The authors declare no competing financial interest.

■ ACKNOWLEDGMENTS

We acknowledge the financial support for this work by the National Science Foundation, USA (Grants CHE 1058373 and CHE-0848171). Any opinions, findings, and conclusions or recommendations expressed in this material are those of the authors and do not necessarily reflect the views of the National Science Foundation. The authors also acknowledge technical assistance from Brian Tabaczynski, Veronica Colón, and Nathan Guterry. The authors thank Dr. David Watson for use of the spectrometers, and Ree Dolnick (RPCI Flow Image Cytometry Facility) for assistance with confocal microscopy. We acknowledge Dionex Corporation for the generous donation of an analytical anion-exchange column.

■ REFERENCES

(1) Liu, H.; Ye, T.; Mao, C. Fluorescent Carbon Nanoparticles Derived from Candle Soot. *Angew. Chem., Int. Ed.* **2007**, *46*, 6473–6475.

(2) Vinci, J. C.; Colón, L. A. Fractionation of Carbon-Based Nanomaterials by Anion-Exchange HPLC. *Anal. Chem.* **2012**, *84*, 1178–1183.

(3) Baker, J. S.; Colón, L. A. Influence of Buffer Composition on the Capillary Electrophoretic Separation of Carbon Nanoparticles. *J. Chromatogr. A* **2009**, *1216*, 9048–9054.

(4) Liu, C.; Zhang, P.; Tian, F.; Li, W.; Li, F.; Liu, W. One-Step Synthesis of Surface Passivated Carbon Nanodots by Microwave Assisted Pyrolysis for Enhanced Multicolor Photoluminescence and Bioimaging. *J. Mater. Chem.* **2011**, *21*, 13163–13167.

(5) Peng, H.; Travas-Sejdic, J. Simple Aqueous Solution Route to Luminescent Carbogenic Dots from Carbohydrates. *Chem. Mater.* **2009**, *21*, 5563–5565.

(6) Qiao, Z.-A.; Wang, Y.; Gao, Y.; Li, H.; Dai, T.; Liu, Y.; Huo, Q. Commercially Activated Carbon As the Source for Producing Multicolor Photoluminescent Carbon Dots by Chemical Oxidation. *Chem. Commun.* **2010**, *46*, 8812–8814.

(7) Dong, Y.; Zhou, N.; Lin, X.; Lin, J.; Chi, Y.; Chen, G. Extraction of Electrochemiluminescent Oxidized Carbon Quantum Dots from Activated Carbon. *Chem. Mater.* **2010**, *22*, 5895–5899.

(8) Wang, Q.; Zheng, H.; Long, Y.; Zhang, L.; Gao, M.; Bai, W. Microwave–Hydrothermal Synthesis of Fluorescent Carbon Dots from Graphite Oxide. *Carbon* **2011**, *49*, 3134–3140.

(9) Zheng, H.; Wang, Q.; Long, Y.; Zhang, H.; Huang, X.; Zhu, R. Enhancing the Luminescence of Carbon Dots with a Reduction Pathway. *Chem. Commun.* **2011**, *47*, 10650–10652.

(10) Song, Y.; Shi, W.; Chen, W.; Li, X.; Ma, H. Fluorescent Carbon Nanodots Conjugated with Folic Acid for Distinguishing Folate-Receptor-Positive Cancer Cells from Normal Cells. *J. Mater. Chem.* **2012**, *22*, 12568–12573.

(11) Baker, S. N.; Baker, G. A. Luminescent Carbon Nanodots: Emergent Nanolights. *Angew. Chem., Int. Ed.* **2010**, *49*, 6726–6744.

(12) Ponomarenko, L. A.; Schedin, F.; Katsnelson, M. I.; Yang, R.; Hill, E. W.; Novoselov, K. S.; Geim, A. K. Chaotic Dirac Billiard in Graphene Quantum Dots. *Science* **2008**, *320*, 356–358.

(13) Fujii, S.; Enoki, T. Cutting of Oxidized Graphene into Nanosized Pieces. *J. Am. Chem. Soc.* **2010**, *132*, 10034–10041.

(14) Li, X.; Wang, X.; Zhang, L.; Lee, S.; Dai, H. Chemically Derived, Ultrasmooth Graphene Nanoribbon Semiconductors. *Science* **2008**, *319*, 1229–1232.

(15) Zhu, S.; Zhang, J.; Qiao, C.; Tang, S.; Li, Y.; Yuan, W.; Li, B.; Tian, L.; Liu, F.; Hu, R.; et al. Strongly Green-Photoluminescent Graphene Quantum Dots for Bioimaging Applications. *Chem. Commun.* **2011**, *47*, 6858–6860.

(16) Tetsuka, H.; Asahi, R.; Nagoya, A.; Okamoto, K.; Tajima, I.; Ohta, R.; Okamoto, A. Optically Tunable Amino-Functionalized Graphene Quantum Dots. *Adv. Mater.* **2012**, *24*, 5333−5338.
(17) Zhang, M.; Bai, L.; Shang, W.; Xie, W.; Ma, H.; Fu, Y.; Fang, D.; Sun, H.; Fan, L.; Han, M.; et al. Facile Synthesis of Water-Soluble, Highly Fluorescent Graphene Quantum Dots As a Robust Biological Label for Stem Cells. *J. Mater. Chem.* **2012**, *22*, 7461−7467.
(18) Tang, L.; Ji, R.; Cao, X.; Lin, J.; Jiang, H.; Li, X.; Teng, K. S.; Luk, C. M.; Zeng, S.; Hao, J.; et al. Deep Ultraviolet Photoluminescence of Water-Soluble Self-Passivated Graphene Quantum Dots. *ACS Nano* **2012**, *6*, 5102−5110.
(19) Wang, F.; Pang, S.; Wang, L.; Li, Q.; Kreiter, M.; Liu, C.-y. One-Step Synthesis of Highly Luminescent Carbon Dots in Noncoordinating Solvents. *Chem. Mater.* **2010**, *22*, 4528−4530.
(20) Yang, S.-T.; Wang, X.; Wang, H.; Lu, F.; Luo, P. G.; Cao, L.; Meziani, M. J.; Liu, J.-H.; Liu, Y.; Chen, M.; et al. Carbon Dots as Nontoxic and High-Performance Fluorescence Imaging Agents. *J. Phys. Chem. C* **2009**, *113*, 18110−18114.
(21) Tian, L.; Ghosh, D.; Chen, W.; Pradhan, S.; Chang, X.; Chen, S. Nanosized Carbon Particles From Natural Gas Soot. *Chem. Mater.* **2009**, *21*, 2803−2809.
(22) Li, H.; He, X.; Kang, Z.; Huang, H.; Liu, Y.; Liu, J.; Lian, S.; Tsang, C. H. A.; Yang, X.; Lee, S.-T. Water-Soluble Fluorescent Carbon Quantum Dots and Photocatalyst Design. *Angew. Chem., Int. Ed.* **2010**, *49*, 4430−4434.
(23) Shen, J.; Zhu, Y.; Yang, X.; Zong, J.; Zhang, J.; Li, C. One-Pot Hydrothermal Synthesis of Graphene Quantum Dots Surface-Passivated by Polyethylene Glycol and Their Photoelectric Conversion under near-Infrared Light. *New J. Chem.* **2012**, *36*, 97−101.
(24) Bourlinos, A. B.; Stassinopoulos, A.; Anglos, D.; Zboril, R.; Karakassides, M.; Giannelis, E. P. Surface Functionalized Carbogenic Quantum Dots. *Small* **2008**, *4*, 455−458.
(25) Bourlinos, A. B.; Zbořil, R.; Petr, J.; Bakandritsos, A.; Krysmann, M.; Giannelis, E. P. Luminescent Surface Quaternized Carbon Dots. *Chem. Mater.* **2011**, *24*, 6−8.
(26) Liu, Y.; Liu, C.-y.; Zhang, Z.-y. Synthesis and Surface Photochemistry of Graphitized Carbon Quantum Dots. *J. Colloid Interface Sci.* **2011**, *356*, 416−421.
(27) Li, Q.; Ohulchanskyy, T. Y.; Liu, R.; Koynov, K.; Wu, D.; Best, A.; Kumar, R.; Bonoiu, A.; Prasad, P. N. Photoluminescent Carbon Dots as Biocompatible Nanoprobes for Targeting Cancer Cells in Vitro. *J. Phys. Chem. C* **2010**, *114*, 12062−12068.
(28) Li, Y.; Hu, Y.; Zhao, Y.; Shi, G.; Deng, L.; Hou, Y.; Qu, L. An Electrochemical Avenue to Green-Luminescent Graphene Quantum Dots as Potential Electron-Acceptors for Photovoltaics. *Adv. Mater.* **2011**, *23*, 776−780.
(29) Shinde, D. B.; Pillai, V. K. Electrochemical Preparation of Luminescent Graphene Quantum Dots from Multiwalled Carbon Nanotubes. *Chem.—Eur. J.* **2012**, *18*, 12522−12528.
(30) Peng, J.; Gao, W.; Gupta, B. K.; Liu, Z.; Romero-Aburto, R.; Ge, L.; Song, L.; Alemany, L. B.; Zhan, X.; Gao, G.; et al. Graphene Quantum Dots Derived from Carbon Fibers. *Nano Lett.* **2012**, *12*, 844−849.
(31) Dong, Y.; Shao, J.; Chen, C.; Li, H.; Wang, R.; Chi, Y.; Lin, X.; Chen, G. Blue luminescent graphene quantum dots and graphene oxide prepared by tuning the carbonization degree of citric acid. *Carbon* **2012**, *50*, 4738−4743.
(32) Wang, X.; Cao, L.; Yang, S.-T.; Lu, F.; Meziani, M. J.; Tian, L.; Sun, K. W.; Bloodgood, M. A.; Sun, Y.-P. Bandgap-Like Strong Fluorescence in Functionalized Carbon Nanoparticles. *Angew. Chem., Int. Ed.* **2010**, *49*, 5310−5314.
(33) Li, L.-s.; Yan, X. Colloidal Graphene Quantum Dots. *J. Phys. Chem. Lett.* **2010**, *1*, 2572−2576.
(34) Sun, X.; Liu, Z.; Welsher, K.; Robinson, J.; Goodwin, A.; Zaric, S.; Dai, H. Nano-Graphene Oxide for Cellular Imaging and Drug Delivery. *Nano Res.* **2008**, *1*, 203−212.
(35) Yu, P.; Wen, X.; Toh, Y.-R.; Tang, J. Temperature-Dependent Fluorescence in Carbon Dots. *J. Phys. Chem. C* **2012**, *116*, 25552−25557.
(36) Yan, X.; Li, B.; Cui, X.; Wei, Q.; Tajima, K.; Li, L.-s. Independent Tuning of the Band Gap and Redox Potential of Graphene Quantum Dots. *J. Phys. Chem. Lett.* **2011**, *2*, 1119−1124.
(37) Li, M.; Wu, W.; Ren, W.; Cheng, H.-M.; Tang, N.; Zhong, W.; Du, Y. Synthesis and Upconversion Luminescence of N-Doped Graphene Quantum Dots. *Appl. Phys. Lett.* **2012**, *101*, 1031071−1031073.
(38) Shen, R.; Song, K.; Liu, H.; Li, Y.; Liu, H. Fluorescence Enhancement and Radiolysis of Carbon Dots through Aqueous γ Radiation Chemistry. *J. Phys. Chem. C* **2012**, *116*, 15826−15832.
(39) Yan, Y.; Liang, Q.-F.; Zhao, H.; Wu, C.-Q. Thermoelectric Properties of Hexagonal Graphene Quantum Dots. *Phys. Lett. A* **2012**, *376*, 1154−1158.
(40) Desai, N. Challenges in Development of Nanoparticle-Based Therapeutics. *AAPS J.* **2012**, *14*, 282−295.
(41) Luo, J.; Cote, L. J.; Tung, V. C.; Tan, A. T. L.; Goins, P. E.; Wu, J.; Huang, J. Graphene Oxide Nanocolloids. *J. Am. Chem. Soc.* **2010**, *132*, 17667−17669.
(42) Xu, X.; Ray, R.; Gu, Y.; Ploehn, H. J.; Gearheart, L.; Raker, K.; Scrivens, W. A. Electrophoretic Analysis and Purification of Fluorescent Single-Walled Carbon Nanotube Fragments. *J. Am. Chem. Soc.* **2004**, *126*, 12736−12737.
(43) Wang, Z.; Lu, M.; Wang, X.; Yin, R.; Song, Y.; Le, X. C.; Wang, H. Quantum Dots Enhanced Ultrasensitive Detection of DNA Adducts. *Anal. Chem.* **2009**, *81*, 10285−10289.